



Abstract

Use of Infrared Thermography for Inspection of Tensile Deformation of Ti-25Nb-0.5O and Ti-25Nb-0.5N Shape Memory Alloys [†]

Karol M. Golasiński ^{1,*} , Michał Maj ² , Sandra Musiał ², Wataru Tasaki ³ and Hee Young Kim ³

¹ Multidisciplinary Research Center, Cardinal Stefan Wyszyński University in Warsaw, 1 Marii Konopnickiej Str., 05-092 Dziekanów Leśny, Poland

² Institute of Fundamental Technological Research, Polish Academy of Sciences, 5b Adolfa Pawińskiego Str., 02-106 Warsaw, Poland; mimaj@ippt.pan.pl (M.M.); smusial@ippt.pan.pl (S.M.)

³ Department of Materials Science, Institute of Pure and Applied Sciences, University of Tsukuba, Tsukuba 305-8573, Japan; tasaki.wataru.rd@gmail.com (W.T.); heeykim@ims.tsukuba.ac.jp (H.Y.K.)

* Correspondence: k.golasinski@uksw.edu.pl

[†] Presented at the 18th International Workshop on Advanced Infrared Technology and Applications (AITA 2025), Kobe, Japan, 15–19 September 2025.

Keywords: shape memory alloys; interstitials; infrared thermography; digital image correlation

The stress- or temperature-induced martensitic transformation from the cubic β phase to the orthorhombic α'' phase is responsible for superelasticity or a shape memory effect in Ni-free Ti-based shape memory alloys (SMAs) [1,2]. However, the addition of oxygen and nitrogen interstitials changes the tensile characteristics of these SMAs [3–5]. For instance, the Ti–25Nb (at.%) SMA exhibits a shape memory effect and a Lüders-type deformation, whereas oxygen-added Ti–25Nb-based SMAs present different but still inhomogeneous superelastic deformation [6]. The goal of this work is to compare the thermomechanical behavior of two SMAs, with compositions Ti–25Nb–0.5O and Ti–25Nb–0.5N, subjected to load–unload tension.

The alloys were prepared by an Ar arc melting method using pre-melted sponges of Ti (purity: >99.7%) and pure Nb (purity: 99.9%). The oxygen and nitrogen concentrations of the alloys were adjusted by amounts of TiO₂ and TiN powders (purity: 99.9%), respectively. Further processing included selected heat treatments and cold rolling, specified in [1]. The load–unload tension was performed using an MTS 858 testing machine (MTS SYSTEMS CORPORATION, Eden Prairie, MN, USA) at a strain rate of around 0.02 1/s. The gauge area of the specimen was 6 mm × 4 mm. During the experiments, a mid-wave infrared camera FLIR Phoenix (Teledyne FLIR LLC, Wilsonville, OR, USA), with high thermal sensitivity up to 0.02 K and a recording frequency of 200 Hz, was used to investigate thermal effects accompanying the deformation of the Ti–25Nb–0.5O and Ti–25Nb–0.5N SMAs. Simultaneously, a sCMOS PCO Edge 5.5 camera (Excelitas Technologies Corp., Pittsburgh, PA, USA) was used to record a sequence in a visible spectrum for further processing using digital image correlation (DIC) to determine the kinematic fields of these alloys in tension. The camera settings were as follows: an image size of 931 pixels × 1280 pixels, with the pixel size equal to 7.7 μ m, and the recording frequency of the camera was equal to 100 Hz. An open-source 2D digital image correlation program, Thermocorr, was also used to couple temperature fields. More details on the methodology are provided in [7]. Examples of the experimental results obtained for Gum Metal (Ti–23Nb–0.7Ta–2.0Zr–1.2O; at.%) using this approach can be found in [8,9].



Academic Editors: Takahide Sakagami and Hirotugu Inoue

Published: 12 September 2025

Citation: Golasiński, K.M.; Maj, M.; Musiał, S.; Tasaki, W.; Kim, H.Y. Use of Infrared Thermography for Inspection of Tensile Deformation of Ti–25Nb–0.5O and Ti–25Nb–0.5N Shape Memory Alloys. *Proceedings* **2025**, *129*, 76. <https://doi.org/10.3390/proceedings2025129076>

Copyright: © 2025 by the authors. Licensee MDPI, Basel, Switzerland. This article is an open access article distributed under the terms and conditions of the Creative Commons Attribution (CC BY) license (<https://creativecommons.org/licenses/by/4.0/>).

The temperature ΔT and strain ε_{yy} fields of Ti-25Nb-0.5O and Ti-25Nb-0.5N SMAs under load–unload tension captured at specific stages of deformation identified in the stress and temperature change vs. strain curves are shown in Figures 1a and 1b, respectively. The stress–strain plots of the Ti-25Nb-0.5O and Ti-25Nb-0.5N SMAs show hysteretic behaviors characterized by superelasticity with the same recovery strains of $\varepsilon_r = 2\%$. However, the hysteresis loop is notably narrower in the case of the Ti-25Nb-0.5N SMA. The letters marked in the stress and temperature vs. strain curves correspond to the following instants of tension: $A_{O/N}$ and $A^*_{O/N}$ —stress σ_{tr} at minimum temperature ΔT_{min} ; $B_{O/N}$ and $B^*_{O/N}$ —maximum stress σ_{max} and maximum temperature ΔT_{max} ; $C_{O/N}$ and $C^*_{O/N}$ — $\sigma = 0$ MPa and temperature after unloading ΔT_{un} . Subscripts O and N refer to those SMAs doped with oxygen and nitrogen, respectively. During loading, first, the average temperature decreases due to the thermoelastic effect $0 \rightarrow A^*_{O/N}$, and, with further loading, the temperature significantly increases due to the forward stress-induced phase transformation $A^*_{O/N} \rightarrow B^*_{O/N}$. In the case of SMAs, ΔT_{min} can be an indicator of the transformation stress σ_{tr} . During unloading, first, the temperature significantly decreases due to the reverse stress-induced phase transformation, and, at the final stage, the temperature slightly increases due to the thermoelastic effect $B^*_{O/N} \rightarrow C^*_{O/N}$.

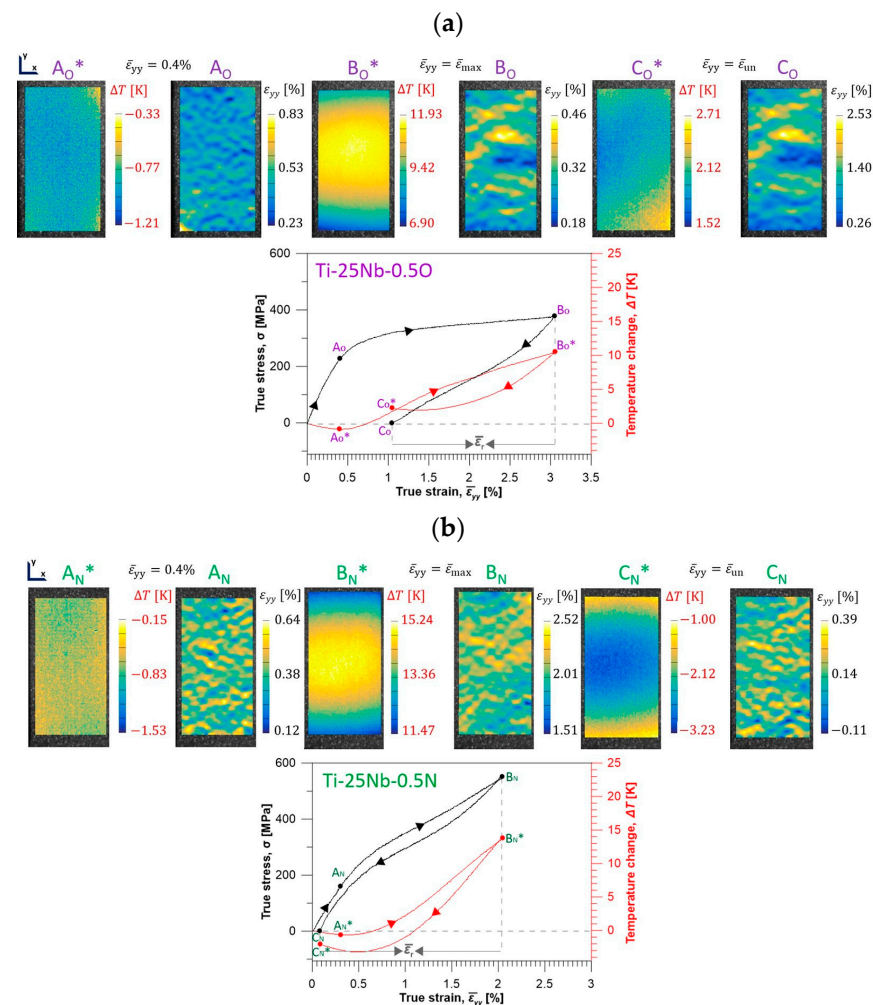


Figure 1. Temperature ΔT and strain ε_{yy} fields of (a) Ti-25Nb-0.5O and (b) Ti-25Nb-0.5N SMAs under load–unload tension at specific stages of deformation selected in the stress and temperature change vs. strain curves.

Although the strain rate applied during the experiments was relatively high to imitate adiabatic conditions, the heat exchange with the surroundings could slightly affect the re-

sults. Moreover, the aforementioned deformation mechanisms are believed to be dominant during specific stages of tension. However, in this class of alloys, deformation twinning could also occur, especially in the final stage of loading, similarly to other metastable β -Ti alloys [10].

The critical parameters identified based on the stress and temperature change vs. strain curves of the Ti-25Nb-0.5O and Ti-25Nb-0.5N SMAs are listed in Table 1. They include transformation stress σ_{tr} at minimum temperature ΔT_{min} , as well as temperature increase during loading ΔT_{eH} and temperature decrease ΔT_{eC} during unloading.

Table 1. Critical parameters identified based on the stress and temperature change vs. strain curves of the Ti-25Nb-0.5O and Ti-25Nb-0.5N SMAs.

Composition	Minimum Temperature, ΔT_{min}	Transformation Stress, σ_{tr}	Temperature Increase, ΔT_{eH}	Temperature Decrease, ΔT_{eC}
Ti-25Nb-0.5O	−0.89 K	236 MPa	11.34 K	8.42 K
Ti-25Nb-0.5N	−0.66 K	204 MPa	14.63 K	16.32 K

The temperature ΔT and strain ε_{yy} fields captured at selected instants of tension demonstrate that the deformation process was inhomogeneous. The maximum local values of ΔT_{max} and ε_{yy_max} , determined at $B^*_{O/N}$ and $B_{O/N}$, respectively, are provided in Table 2.

Table 2. Maximum local values of ΔT_{max} and ε_{yy_max} determined at $B^*_{O/N}$ and $B_{O/N}$.

Composition	Maximum Local Temperature, ΔT_{max}	Maximum Local Strain, ε_{yy_max}
Ti-25Nb-0.5O	11.93 K	4.6
Ti-25Nb-0.5N	15.24 K	2.5

The values of ΔT_{max} were rather close to those of ΔT_{eH} . However, the values of ε_{yy_max} were quite higher than those of ε_r .

Our results show that infrared thermography is a useful technique to track the peculiar temperature changes of the Ti-25Nb-0.5O and Ti-25Nb-0.5N SMAs. The temperature fields captured at selected stages of loading revealed heat sources associated with the deformation process. The thermal effects were discussed in view of the kinematic characteristics obtained using DIC. It was shown that temperature changes can serve to identify particular deformation stages of the SMAs considered in this study.

Author Contributions: Conceptualization, K.M.G. and H.Y.K.; methodology, K.M.G., M.M., S.M., W.T. and H.Y.K.; software, K.M.G., M.M. and S.M.; validation, K.M.G.; formal analysis, K.M.G., M.M. and S.M.; investigation, K.M.G., M.M. and S.M.; resources, K.M.G. and H.Y.K.; data curation, K.M.G., M.M. and S.M.; writing—original draft preparation, K.M.G.; writing—review and editing, K.M.G.; visualization, K.M.G., M.M. and S.M.; supervision, H.Y.K.; project administration, K.M.G.; funding acquisition, K.M.G. All authors have read and agreed to the published version of the manuscript.

Funding: This research was funded by the National Science Centre, Poland, through the Grant 2023/48/C/ST8/00038.

Institutional Review Board Statement: Not applicable.

Informed Consent Statement: Not applicable.

Data Availability Statement: The data supporting the findings of this study are openly available in Zenodo at <https://doi.org/10.5281/zenodo.17349659>.

Acknowledgments: The authors would like to express their gratitude to Leszek Urbański from the Institute of Fundamental Technological Research, Polish Academy of Sciences for conducting tensile tests and his diligent efforts in data collection as well as processing.

Conflicts of Interest: The authors declare no conflicts of interest. The funders had no role in the design of the study; in the collection, analyses, or interpretation of data; in the writing of the manuscript; or in the decision to publish the results.

References

1. Kim, H.Y.; Satoru, H.; Kim, J.I.; Hosoda, H.; Miyazaki, S. Mechanical properties and shape memory behavior of Ti-Nb alloys. *Mater. Trans.* **2004**, *45*, 2443–2448. [\[CrossRef\]](#)
2. Kim, H.Y.; Ikehara, Y.; Kim, J.I.; Hosoda, H.; Miyazaki, S. Martensitic transformation, shape memory effect and superelasticity of Ti-Nb binary alloys. *Acta Mater.* **2006**, *54*, 2419–2429. [\[CrossRef\]](#)
3. Tahara, M.; Kim, H.Y.; Inamura, T.; Hosoda, H.; Miyazaki, S. Role of interstitial atoms in the microstructure and non-linear elastic deformation behavior of Ti-Nb alloy. *J. Alloys Compd.* **2013**, *577*, S404–S407. [\[CrossRef\]](#)
4. Tahara, M.; Kim, H.Y.; Hosoda, H.; Miyazaki, S. Shape memory effect and cyclic deformation behavior of Ti-Nb-N alloys. *Funct. Mater. Lett.* **2009**, *2*, 79–82. [\[CrossRef\]](#)
5. Miyazaki, S. My Experience with Ti-Ni-Based and Ti-Based Shape Memory Alloys. *Shape Mem. Superelasticity* **2017**, *3*, 279–314. [\[CrossRef\]](#)
6. Golasiński, K.; Maj, M.; Tasaki, W.; Pieczyska, E.A.; Kim, H.Y. Full-Field Deformation Study of Ti-25Nb, Ti-25Nb-0.3O and Ti-25Nb-0.7O Shape Memory Alloys During Tension Using Digital Image Correlation. *Metall. Mater. Trans. A* **2024**, *55*, 2509–2518. [\[CrossRef\]](#)
7. Nowak, M.; Maj, M. Determination of coupled mechanical and thermal fields using 2D digital image correlation and infrared thermography: Numerical procedures and results. *Archiv. Civ. Mech. Eng.* **2018**, *18*, 630–644. [\[CrossRef\]](#)
8. Golasiński, K.M.; Pieczyska, E.A.; Staszczak, M.; Maj, M.; Furuta, T.; Kuramoto, S. Infrared thermography applied for experimental investigation of thermomechanical couplings in Gum Metal. *Quant. InfraRed Thermogr. J.* **2017**, *14*, 226–233. [\[CrossRef\]](#)
9. Golasiński, K.M.; Maj, M.; Urbański, L.; Staszczak, M.; Gradys, A.; Pieczyska, E.A. Experimental study of thermomechanical behaviour of Gum Metal during cyclic tensile loadings: The quantitative contribution of IRT and DIC. *Quant. InfraRed Thermogr. J.* **2023**, *21*, 259–276. [\[CrossRef\]](#)
10. Tobe, H.; Kim, H.Y.; Inamura, T.; Hosoda, H.; Miyazaki, S. Origin of {332} twinning in metastable β -Ti alloys. *Acta Mater.* **2014**, *64*, 345–355. [\[CrossRef\]](#)

Disclaimer/Publisher’s Note: The statements, opinions and data contained in all publications are solely those of the individual author(s) and contributor(s) and not of MDPI and/or the editor(s). MDPI and/or the editor(s) disclaim responsibility for any injury to people or property resulting from any ideas, methods, instructions or products referred to in the content.